

C.M. Henze and M.B. Bragg, "**Turbulence Intesity Measurements Tecnique for Use in Icing Wind Tunnels**", Journal of Aircraft Vol 36, No. 2, March-April 1999.

A Turbulence Intensity Measurement Technique for use in Icing Wind Tunnels

Chad M. Henze* and Michael B. Bragg[†]
University of Illinois at Urbana-Champaign
Urbana, IL

Abstract

Current understanding of the ice accretion process is based largely on icing wind tunnel tests. Wind tunnel turbulence has been identified as having potentially important effects on the results of tests performed in icing tunnels. The turbulence intensity level in icing tunnels in the absence of the spray cloud had been previously measured and found to be quite high due to the lack of turbulence reducing screens, and to the presence of the spray system in the settling chamber. However, the turbulence intensity level in the presence of the spray cloud had not been measured. In this study, a method for making such measurements was developed and a limited set of turbulence measurements was taken in the NASA Lewis Icing Research Tunnel. Turbulent velocity fluctuations were measured using hot-wire sensors. Droplets striking the wire resulted in distinct spikes in the hot-wire voltage that were removed using a digital acceleration threshold filter. The remaining data were used to calculate the turbulence intensity. Using this method, the turbulence intensity level in the Icing Research Tunnel was found to be highly dependent on nozzle air pressure, while other factors such as nozzle water pressure, droplet size, and cloud liquid water content had little effect.

* Graduate Research Assistant, Department of Aeronautical and Astronautical Engineering, currently Analytical Engineer, Hamilton Standard, MS 1-3-BC52, One Hamilton Road, Windsor Locks, CT 06096, member AIAA.

Introduction

Wind tunnel testing continues to play an important role in research to improve the understanding of the physical processes behind ice accretion and its effects on aircraft performance. While wind tunnel testing is an invaluable tool, there will always be important differences between the wind tunnel environment and that which an aircraft experiences in flight. One problem of particular importance is the turbulent fluctuations in wind tunnel flows, which are often significantly larger than those in the atmosphere. The influence of free-stream turbulence is important in the study of aircraft icing since turbulence in icing wind tunnels is inherently high due to the lack of anti-turbulence screens, and the turbulence generated by the spray apparatus. These fluctuations are commonly measured in terms of turbulence intensity, which is defined as the standard deviation of the velocity normalized by the mean velocity. Gonzalez¹ measured turbulence levels in the NASA Lewis Icing Research Tunnel (IRT) ranging from approximately 0.4% to 1.0% for test-section velocities between 50 and 200 mph. With the nozzle spray air (no water) operating, he saw even higher turbulence levels which varied from between 3 and 4% at low speeds to about 1% for test section velocities of 200 mph. In similar measurements, Poinatte² found turbulence levels in the IRT ranging from 0.5-0.7% over a range of 70 to 210 mph without the spray nozzle air operating. He also measured higher levels with the nozzle air (no water) on, but these values weren't reported due to concerns about temperature fluctuations from the heated nozzle air. In contrast, taking hot-wire measurements in flight, Poinatte² measured turbulence intensity levels of less than 0.1% in clear air.

[†] Professor, Department of Aeronautical and Astronautical Engineering, 306 Talbot Laboratory, 104 South

The role of free-stream turbulence in the ice accretion process is not well understood. While there are several possible ways in which increased velocity fluctuations could affect the accretion of ice, it seems likely that enhancement of heat transfer in the region of ice growth would play the most important role.

Gelder and Lewis³ and Poinsett² have made comparisons of heat transfer on an airfoil in flight and in the IRT. Gelder and Lewis found an increase in heat transfer of as much as 30% in the IRT. Poinsett's more recent investigation of heat transfer from an NACA 0012 found a maximum heat transfer increase in the IRT of 10% over heat transfer in flight. These studies indicate that the tunnel environment has a significant effect on heat transfer. This increased heat transfer is likely due to increased turbulence, and it is logical that such increased heat transfer would affect ice accretion. It is thus important to characterize the turbulence level in flight icing conditions and icing wind tunnels.

While hot-wire anemometry is the most popular method for measuring turbulent fluctuations, the icing environment presents a particular problem in the use of this technique. The presence of the water droplets has a significant effect on the hot-wire signal. In order to successfully measure turbulence in these conditions, a method must be developed for separating the effects of droplets striking the wire from the turbulent fluctuations in the free stream. Several researchers^{4,8} have used hot-wire anemometry to make measurements in flows containing liquid droplets by noting that there is a distinct spike in the hot-wire signal when a droplet strikes the wire. By removing such spikes, Hetsroni, Cutler, and Sokolov⁷ were able to successfully measure mean velocities and turbulent velocity fluctuations.

Wright St., Urbana, IL 61801, Associate Fellow AIAA.

Hetsroni and Sokolov⁸ made some important observations when they applied this method to two-phase turbulent jet flow with droplet sizes and airspeeds similar to the icing tunnel case. They noted that the droplets were almost immediately swept off the wire and the signal returned quickly to the initial heat transfer level. They also observed that some small droplets caused signal fluctuations that were only slightly greater than those due to velocity fluctuations, and thus fell under the threshold voltage. However, they assumed that in general the signals due to droplet strikes were much higher than those due to turbulent fluctuations. Farrar et.al.,⁹ in a study of air bubbles in a liquid flow, also observed that the passing of some small bubbles was difficult to detect. However, they found that these small bubbles were much more clearly identified if they applied the filter to the derivative of the hot-wire voltage. Ritsch and Davidson¹⁰ successfully applied a similar threshold technique to the time derivative of the signal from a flow containing small particles. They also noted that a high data rate was necessary to detect the rapid phase changes.

It is important to characterize the turbulence level in icing tunnels due to the potential impact on ice accretion. However, the measurement of turbulence intensity using hot-wire anemometry in droplet cloud conditions is complicated by the effects of the water droplets on the anemometer signal. The fluctuations in the anemometer signal due to droplet strikes have to be filtered from the data if accurate turbulence measurements are to be made. The development of such a filter is outlined here. Tests conducted in the University of Illinois Subsonic Aerodynamics Research Laboratory and in the Icing Research Tunnel at NASA Lewis Research Center were used as the basis of the filter development. The results of the data taken in the IRT to support the development of the filtering method also provided some

preliminary insight into the turbulence characteristics in the icing cloud of the IRT and are presented here.

Experimental Method Development

This section presents the development of the experimental method used to measure the turbulence level in the presence of the spray cloud in the IRT. The filtering technique used to remove droplet strikes from the hot-wire signal will be described first. Two corrections to the measured turbulence intensity levels will then be discussed, and finally the resulting turbulence measurement method will be summarized.

Data Acquisition and Reduction

The hot-wire anemometry system used was a TSI Incorporated IFA100. The hot-wire probes chosen were TSI model 1210 general-purpose probes. The 1.27 mm long wires on these probes were platinum coated tungsten with diameters of 3.8 or 5.1 microns. The hot-wire sensors were calibrated in a small wind tunnel at the University of Illinois. A Pentium PC with an analog to digital data-acquisition board was used to acquire data from the anemometer. The probes were operated in the end-flow orientation in order to measure axial turbulence intensity. The data were acquired at an acquisition rate of 100 kHz in the droplet cloud in order to resolve the spikes in the signal due to droplet strikes. Through the use of signal conditioners, both DC and high-pass filtered hot-wire signals were recorded to obtain the mean and fluctuating velocity, respectively. For a more complete description of the data acquisition methods and wind-tunnel facilities used see Henze.¹¹

Prior to being converted to velocities, the hot-wire voltages were corrected for the difference between the ambient temperature at the time of data acquisition, and the ambient temperature at which the wire was calibrated. Velocities were then calculated from these temperature-corrected voltages by means of a calibration polynomial. The temperature-corrected velocities were then corrected for differences in the air density at calibration and acquisition. The turbulence intensity was then calculated. For measurements acquired in the spray cloud of the icing wind tunnel, the droplet filter and corrections for the effects of the probe shield and the heated nozzle air were applied. These corrections and filtering technique are described in the following sections. These data reduction methods are also explained in detail in Henze.¹¹

Droplet Filtering Technique

An acceleration threshold method was developed for identifying the droplet strikes in the hot-wire data. The term “threshold method” refers to removing data that exceed some preset level in a measured or derived quantity. The following explanation of this filtering method will rely on the time traces of velocity and acceleration data shown in Figs. 1 and 2. The calculated velocities and accelerations presented in these plots were not actual velocities or accelerations when a droplet struck the wire, but were the acceleration or velocity calculated based on the hot-wire calibration in air alone. The high heat transfer due to the water leads to unrealistically large “sensed” velocities and accelerations, which can be removed using a threshold filter. Figure 1 is a 0.01-second time trace, while Fig. 2 is a plot of a 0.002-second segment of the same data. Time traces for the same conditions with no

water present were also plotted for comparison. The importance of using an acceleration threshold filter as opposed to a velocity threshold, as noted by Farrar et al.⁹ in their work in bubbly flows, was apparent in these time traces. While the larger spikes due to droplets were clearly apparent in the velocity plots, some of the smaller spikes, apparently due to small drops or partial droplet strikes, were difficult to differentiate from free-stream turbulence. Plotting the accelerations made even the smaller spikes considerably more apparent, and thus much easier to filter using a threshold method.

The acceleration threshold filtering method used is illustrated in Fig. 3. An upper and lower threshold, indicated by the two horizontal lines, was set just above the maximum absolute acceleration of a corresponding data set with the nozzle air operating at the appropriate pressure, but no water present. At 100 mph, a threshold level of 100,000 ft/s² was found to be appropriate for nearly all cases. When any acceleration value exceeded the threshold, it was considered to be part of a droplet impingement generated spike. That sample along with all data points 0.0001 seconds (10 points in the case of data acquired at 100kHz) before and after it were then marked to be excluded from the turbulence intensity calculations. These additional points were removed to avoid the remaining “stumps” of the droplets spikes noted by Hetsroni, Cutler, and Sokolov.⁷ Dotted lines were used to indicated the excluded points in Fig. 3. It should be noted that the acceleration threshold level and number of data points removed would likely not be appropriate at significantly higher or lower freestream velocities, or for drop sizes outside the range tested. Only a small amount of data was acquired at other velocities during this test. Therefore, no observations concerning appropriate filter settings at other conditions can be made. With the data filtering

complete, the turbulence intensity calculation was then performed on the remaining data. It can also be seen in this plot that some small spikes, apparently indicating small droplet impacts or partial impacts, fell below the threshold and were not filtered. However, in general the acceleration peaks caused by the droplets were much larger than those due to turbulent fluctuations in the air. As an indication that this was the case, for the data from which the time traces in Figs. 1 and 2 were extracted, the magnitude of the maximum acceleration in the no-water case was $8.06 \times 10^4 \text{ ft/s}^2$. In comparison, the maximum sensed acceleration in the water-on case was much higher at almost $1 \times 10^7 \text{ ft/s}^2$.

There was some initial concern that setting such a threshold would essentially set the turbulence intensity by removing not only droplet strikes but any additional fluctuations caused by the injection and presence of the water droplets in the air stream which were not due to the water striking the wire. However, while the maximum acceleration in the water-off data plotted in Figs. 1 and 2, was $80,600 \text{ ft/s}^2$, applying a threshold level as low as $50,000 \text{ ft/s}^2$ to these data only removed 0.617% of the data reducing the turbulence intensity from 0.663% to 0.662%. This indicated that the majority of the accelerations in the water-off data were actually considerably lower than the maximum acceleration and thus considerably lower than the threshold level. Assuming that any flow accelerations caused by the spray cloud which weren't due to droplets striking the wire were on the order of the accelerations in the water-off data, then the majority of those accelerations were also well below the threshold.

Figure 4 shows the results of applying the filtering technique to the same data set from which the previous time traces (Figs. 1-3) were extracted. (The turbulence data are uncorrected for heated air and model interference effects to be discussed later.) The

turbulence intensity as a function of the acceleration filter setting is depicted along with the percent of the data removed by the filtering process. The turbulence intensity level for the water-off data is also shown for reference. Note that water-off means the nozzle water pressure was zero and the nozzle air remained at the level required to produce the desired cloud properties for that water-on test condition.

The turbulence intensity level was observed to approach that of the corresponding water-off case as the filter setting was decreased. The maximum acceleration of the water-off data was 8.06×10^4 for this case. At this acceleration filter setting the value of the water-on turbulence intensity was 0.073% greater than the water-off value. At an acceleration filter setting of 5×10^4 the increase above the water-off data was only 0.031%. The amount of data removed from the water-on data set in Fig. 4, approximately 77% at a filter setting of 100,000 ft/s^2 , was quite large. This indicates that the number of detected water strikes was very high for these conditions. However, with the model shield present (see below), applying the filter to data sets where the LWC was lower resulted in far less data being removed.

The filter results shown in Fig. 5 are for the same tunnel conditions as Fig. 4 except that the LWC was 0.9 g/m^3 instead of 1.5 g/m^3 . In this case a filter setting of 100,000 ft/s^2 removed only about 12% of the data and the water-on turbulence level asymptotically approached 0.594% a value slightly larger than the value of 0.555% with no water present. Based on extensive filter setting studies similar to that depicted in Figs. 4 and 5 filter settings near the maximum water-off acceleration level provided consistent and defensible results. Therefore, a value of 1×10^5 , representative of the range of maximum water-off accelerations measured, was chosen as the filter setting for all turbulence data acquired at 100 mph.

Hot-Wire Shielding

In an attempt to shield the hot-wire sensor from the majority of the droplets in the flow, the sensor was placed between the boundary layer and the trajectories of the larger droplets passing above an airfoil at angle of attack as illustrated in Fig. 6. While the majority of the data taken in the IRT were acquired at temperatures above freezing to prevent ice accretion, a small amount of data was acquired in icing conditions. The ice accretion on the probe support during these tests, Fig. 7, revealed that a majority of the water mass in the cloud was indeed being deflected away from the probe by the model. The measured RMS level of the hot-wire signal was seen to decrease with increasing angle of attack, also indicating that the model was serving to shield the sensor. However, after further analysis it was found that while the large droplets in the cloud were being deflected away from the probe, small droplets were still striking the sensor. Droplet trajectory calculations showed that droplets below 12 microns in diameter could potentially strike the sensor. However, because the smaller droplets are orders of magnitude greater in number than the deflected large droplets, the actual number of droplet strikes was not appreciably reduced by the use of the model shield. The fact that the shield reduced the ice accretion at the probe location will be valuable if these measurement techniques are used in icing conditions, either in flight or in the wind tunnel.

Since the data presented in this paper were acquired using the airfoil shield technique, a means for correcting the data for the airfoil-generated turbulence sensed by the probe was developed. To acquire the needed data a wind-tunnel test was conducted at the University of

Illinois' Subsonic Aerodynamics Laboratory. Turbulence intensity measurements were taken with the probe at varying distances from the model surface, with the model at varying angles of attack. Turbulence intensity values due to different sources can be combined as shown in equation 1.¹²

$$TI = \sqrt{TI_1^2 + TI_2^2 + TI_3^2 + \Lambda} \quad (1)$$

In equation 1, TI is the total measured turbulence level, TI_1 , TI_2 , etc., are the turbulence levels from various sources. For the tests performed in the Icing Research Tunnel, the probe was positioned 1.5 inches from the model surface with the model at 8 degrees angle of attack. Using equation 1, and the data from the UIUC tests at these conditions, the average turbulence due to the presence of the model was found to be 0.18%. This value was used to correct the turbulence intensity measurements presented. Note that this correction is only valid at 100 mph with the probe location and model angle of attack used for these tests.

Effects of Heated Nozzle Air

The air exiting the IRT spray nozzles is heated to approximately 180° F to prevent ice from forming in the nozzles. As noted in Poinatte², it is likely that this hot air was causing high-frequency temperature fluctuations that were being misinterpreted as velocity fluctuations and thus contributed to the measured turbulence intensity values in his data.

In order to examine and quantify this effect, identical turbulence measurements were taken at varying nozzle air pressures with and without the nozzle air heated and no water cloud present. As expected, the heating of the nozzle air did cause an increase in the measured turbulence intensities. Larger turbulence values at higher nozzle air pressures

indicated that as more heated air was introduced into the free-stream flow by the nozzles, the temperature fluctuations seen in the test section increased. Based on equation 1, the errors in the turbulence intensity due to the temperature fluctuations were calculated. The turbulence intensity contribution due to the heated nozzle air ranged from 0.2% at 10 psig nozzle air to almost 0.4% at 80 psig and corresponded to temperature fluctuation RMS of approximately 0.3° C. This apparent turbulence intensity due to temperature fluctuations was fit by a polynomial in nozzle air pressure (psig) with a correlation coefficient , $R^2 = 0.97$.

$$TI_{\text{heat}} = 1.55 \times 10^{-6} \cdot P_{\text{air}}^3 - 2.86 \times 10^{-4} \cdot P_{\text{air}}^2 + 1.78 \times 10^{-2} \cdot P_{\text{air}} \quad (2)$$

The results of the measurements taken in the Icing Research Tunnel were corrected using this equation. Note that equation 2 is only valid at 100 mph and the 180°F nozzle air temperature tested. It is also quite likely that these temperature fluctuations are spatially dependent on location relative to a nozzle. This spatial variation was not studied in this test.

Summary of Turbulence Measurement Technique

In order to calculate a turbulence intensity value from the velocity data acquired using the hot-wire sensor, the droplet strike signals were first removed from the corrected velocity data using the threshold filter. The total turbulence intensity was found by calculating the standard deviation of the remaining velocity measurements, normalizing that value by the mean velocity, and multiplying by 100 to express the turbulence intensity as a percent. The effect of the heated nozzle air was then calculated using equation 2. This value along with the correction for the presence of the airfoil shield were then subtracted from the total total turbulence value by arranging equation 1 as shown in equation 3.

$$TI_{\text{final}} = \sqrt{TI_{\text{total}}^2 - TI_{\text{heat}}^2 - TI_{\text{shield}}^2}$$

In this equation TI_{final} is the resulting turbulence level, TI_{total} is the total value calculated from the measured velocities, TI_{heat} is the contribution due to heated nozzle air, and TI_{shield} is the turbulence resulting from the presence of the model shield.

IRT Turbulence Variations Due to Cloud Conditions

While the primary purpose of the icing research tunnel tests was to support the development of the droplet filtering technique described above, some observations concerning the turbulence intensity level in the spray cloud were made. Specifically, the effects of nozzle air and water pressure, and the resulting droplet size and liquid water content were investigated, and those results are presented here.

The effect of the variation of nozzle air pressure on the tunnel turbulence intensity level was examined by acquiring data at varying nozzle air pressures with no water present.

For these measurements, the model was set at 0 degrees angle of attack, and the probe was 6 inches from the model surface, therefore, no correction for the presence of the model was needed. The data were corrected for the heated nozzle air. The results of the tests are shown in Fig. 8. Overall, these water-off turbulence measurements agreed reasonably well with those of other researchers. Poinatte² found turbulence levels of 0.6%, 0.52%, and 0.7% at velocities of 70, 140, and 210 mph respectively with no nozzle air pressure. Gonzalez¹ measured turbulence intensity in the IRT including the spatial variation in the test section. At 100 mph he reported 0.4 to 1.0 % with no nozzle air and 1.0 to 1.5 % with the nozzle air operating at 80 psig. It was apparent that increasing nozzle air pressure caused a significant increase in the tunnel free-stream turbulence level. This was not surprising, as the air from the nozzles entered the free stream with a considerable cross-flow component.

The effect of nozzle water pressure on turbulence level was explored by taking measurements at varying nozzle water and air pressures. The model shield was used in acquiring the data presented here, therefore, the turbulence levels have been corrected for the presence of the model as well as the effects of the heated nozzle air. Analysis of the data was performed using multiple regression analysis to quantify the dependence of turbulence level on nozzle air and water pressure. The analysis resulted in the following equation for the turbulence intensity (%) as a function of nozzle air and water pressure (psig).

$$TI = 0.464 + 0.00493 P_{\text{air}} + 0.000110 P_{\text{water}} \quad (3)$$

The coefficient on the air pressure term in eq. (3) is over 44 times that of the water pressure term, again indicating that turbulence intensity is largely a function of air pressure. For the mod-1 nozzles used in the IRT, a typical cloud of 25 μm droplets requires a nozzle air

pressure of 30 psig, and a nozzle water pressure of approximately 110 psig. At these nozzle pressures and 100 mph, based on eq. (3), the nozzle air pressure contributes 0.15% to the turbulence level, while the nozzle water pressure only results in an increase of 0.012%. The correlation coefficient, R^2 , was 0.83 indicating that eq. (3) does an excellent job of predicting the turbulence intensity values. If LWC and droplet size were also included as independent variables, no improvement in the regression equation was seen. Assuming that turbulence intensity was a function of LWC and drop size alone produced a poor prediction with a correlation coefficient of only 0.346. This analysis clearly indicates that turbulence intensity is dependent on nozzle air pressure and to a lesser extent water pressure with no significant contributions from LWC and droplet size. Note that equation 3 is not intended to be a calibration of the turbulence intensity in the IRT, as data were only acquired at one velocity. It is presented only to demonstrate the relative effects of nozzle air and water pressure on the turbulence level in the spray.

Lines of turbulence intensity vs. nozzle air pressure from the linear regression were plotted in Fig. 9 along with the experimental data used in the regression. The data have been corrected for the presence of the model as well as the effects of the heated nozzle air. The data contain water pressures from 0 to 282.6 psig and the curve fit of eq. (3) was shown for water pressures of 0 and 300psig. The focus of this study was the development of the technique and not the detailed documentation of the water-on turbulence level and flow quality in the icing tunnel. As a result sufficient data was not always available to reduce the uncertainty in the measured turbulence so the regression analysis was used to establish the important influence of air and water pressure. It was clear from Fig. 9 and eq.(3) that icing

tunnel turbulence was predominantly controlled by the nozzle air pressure and water pressure was a small effect.

During testing in the IRT and other icing wind tunnels, specific liquid water content (LWC) and droplet size conditions are set using the nozzle air and water pressures. Therefore, it is possible that trends observed in tunnel-test results where droplet size and LWC are varied could be affected by variations in turbulence intensity due to the varying nozzle air and water pressures required to produce these LWC and droplet size changes. Turbulence intensity data are plotted versus LWC and grouped into three droplet size ranges on Fig. 10. These results were corrected for heated air and model shield effects. The lines on this curve were based on the air and water pressures from the IRT nozzle calibration¹³ required to produce a given droplet size and LWC. Then the multiple regression of eq. (3) was used to determine the tunnel turbulence at these conditions. The general trend that emerged was an increase in turbulence intensity as droplet size decreased and liquid water content increased. The experimental values are seen to be well predicted by the empirically derived lines. These trends agreed with earlier observations since an increase in air pressure causes a decrease in droplet size. Also, as water pressure is increased to increase LWC, nozzle air pressure must also increase to maintain a given droplet size. Based on this, it was apparent that the increased turbulence was primarily due to higher nozzle air pressures that generate higher LWC's and lower droplet sizes.

Summary and Conclusions

The turbulence level in icing wind tunnels is inherently high due to a lack of flow straighteners and turbulence reduction screens, and the presence of the spray bar system. It is reasonable to assume that this increased turbulence intensity has affected the results of tests performed in icing tunnels, although to what extent is unknown. Documentation of the turbulence level in wind tunnels and natural icing clouds is needed to address this problem. However, the presence of the water droplets complicates making such measurements using thermal anemometry – the most common method of measuring turbulence intensity. In this paper a method has been presented which uses an acceleration threshold filter to successfully remove the influence of the droplets from the hot-wire anemometer data.

From this study the following conclusions can be drawn:

1. A hot-wire probe with a digital acceleration filter can be successfully used to measure the turbulence level in an icing tunnel with the water spray on.
2. The airfoil shield reduced the mass of water at the hot-wire sensor location by deflecting the large droplets. If such shielding is used, a small correction in the measured turbulence intensity must be applied due to the airfoil-generated turbulence.
3. The heated nozzle air used to prevent ice formation in the nozzles caused temperature fluctuations that were falsely interpreted as velocity fluctuations. Turbulence data must be corrected to account for this effect unless measurements can be made with the nozzle air at the freestream temperature.
4. At a given velocity, the measured turbulence intensity in the icing tunnel spray cloud was primarily a function of nozzle air pressure. Nozzle water pressure had only a small effect

on the turbulence level. Changes in turbulence level due to LWC and droplet size can be explained in terms of the nozzle air pressure. Turbulence measured in the icing cloud was consistently slightly higher than that measured with no water present at the same nozzle air pressure. However, it is not clear at this time whether this is due to the presence of the droplets, or due to small droplets striking the wire which are not properly removed by the threshold filter.

A more thorough study of the turbulence level in the Icing Research Tunnel and other icing tunnels needs to be performed using techniques similar to those outlined here. These techniques may also be useful in measuring the turbulence levels in natural icing clouds during flight test. Once turbulence levels in icing tunnels and natural icing clouds are known, progress can be made in understanding the influence of tunnel turbulence on the ability of the tunnel to simulate the natural icing environment.

Acknowledgments

This work was supported in part by NASA Lewis Research Center under grant NAG3-1988. The authors would like to thank David Anderson, Simon Chen, Jose Gonzalez and the Icing Research Tunnel staff at NASA Lewis for their assistance during this effort. The authors also acknowledge the assistance of UIUC graduate students Steve Fennel, Andy Broeren, John Winkler, and Sam Lee for their help with the data acquisition and Jonathan Reichhold and Han Kim for their assistance with the data acquisition code.

- ¹ Gonsalez, J.C., and Arrington, E.A., "Aerodynamic Calibration of the NASA Lewis Icing Research Tunnel (1997 Test)," AIAA Paper 98-0633, 36th Aerospace Sciences Meeting and Exhibit, January 12-15, 1998.
- ² Poinsette, P.E., "Heat Transfer Measurements From a NACA 0012 Airfoil in Flight and in the NASA Lewis Research Tunnel," NASA CR-4278, 1990.
- ³ Gelder, T. F., and Lewis, J. P., "Comparison of Heat Transfer From Airfoil in Natural and Simulated Icing conditions," NACA TN 2480, September 1951.
- ⁴ Merceret, F.J., "An Experimental Study to Determine the Utility of Standard Commercial Hot-wire and Coated Wedge-Shaped Hot-film Probes for Measurement of Turbulence in Water-Contaminated Air Flows," Technical Report #40, Chesapeake Bay Institute, The John's Hopkins University, 1968.
- ⁵ Merceret, F.J., "An Experimental Study to Determine the Utility of Standard Commercial Hot-wire and Coated Wedge-Shaped Hot-film Probes for Measurement of Turbulence in Water-Contaminated Air Flows, Part II," Technical Report #50, Chesapeake Bay Institute, The John's Hopkins University, 1969.
- ⁶ Goldschmidt, V.W. and Householder, M.K., "The Hotwire Anemometer as an Aerosol Droplet Size Sampler," *Atmospheric Environment*, Vol. 3, Pergamon Press, 1969, pp. 643-651.
- ⁷ Hetsroni, G., Cutler, J.M., and Sokolov, "Measurements of Velocity and Droplets Concentration in Two-Phase Flows," *Journal of Applied Mechanics, Transactions of the ASME*, June 1969, pp. 334-335.
- ⁸ Hetsroni, G., and Sokolov, "Distribution of Mass, Velocity, and Intensity of Turbulence in a Two-Phase Turbulent Jet," *Journal of Applied Mechanics, Transactions of the ASME*, June 1971, pp. 315-327.
- ⁹ Farrar, B., Samways, A.L., Ali, J., and Bruun, H.H., "A Computer-Based Hot-Film Technique for Two-Phase Flow Measurements," *Meas. Sci. Technol.* 6, 1995, pp 1528-1537.
- ¹⁰ Ritsch, M.L. and Davidson, J.H., "Phase Discrimination in Gas-Particle Flows Using Thermal Anemometry," *Journal of Fluids Engineering, Transactions of the ASME*, Vol. 114, December, 1992, pp. 692-694.
- ¹¹ Henze, C.M., "Turbulence Intensity Measurements in Icing Cloud Conditions," M.S. Thesis, University of Illinois at Urbana-Champaign, Urbana, IL., 1997.
- ¹² Anon., "Temperature Compensation of Thermal Sensors," TSI Technical Bulletin 16.

¹³ Ide, R.F., "Liquid Water Content and Droplet Size Calibration of the NASA Lewis Icing Research Tunnel," NASA TM 104415, 1991.

Figure Titles

Fig. 1 Velocity and acceleration traces. (Drop size = $30 \pm 3\mu\text{m}$, LWC = $1.5 \pm 0.15 \text{ g/m}^3$, velocity = $100 \pm 2.5 \text{ mph}$, velocity $\pm 4.2 \text{ ft/s}$, acceleration $\pm 3.1\%$, time $\pm 0.01\%$)

Fig. 2 Expanded view of velocity and acceleration traces. (Drop size = $30 \pm 3\mu\text{m}$, LWC = $1.5 \pm 0.15 \text{ g/m}^3$, velocity = $100 \pm 2.5 \text{ mph}$, velocity $\pm 4.2 \text{ ft/s}$, acceleration $\pm 3.1\%$, time $\pm 0.01\%$)

Fig. 3 Droplet threshold filter example. (Drop size = $30 \pm 3\mu\text{m}$, LWC = $1.5 \pm .15 \text{ g/m}^3$, velocity = $100 \pm 2.5 \text{ mph}$, acceleration $\pm 3.1\%$, time $\pm 0.01\%$)

Fig. 4 Turbulence intensity and percent data removed as a function of acceleration threshold value. (Drop size = $30 \pm 3\mu\text{m}$, LWC = $1.5 \pm 0.15 \text{ g/m}^3$, velocity = $100 \pm 2.5 \text{ mph}$, turbulence intensity ± 0.04)

Fig. 5 Turbulence intensity and percent data removed as a function of acceleration threshold value. (Drop size = $30 \pm 3\mu\text{m}$, LWC = $1.5 \pm 0.15 \text{ g/m}^3$, velocity = $100 \pm 2.5 \text{ mph}$, turbulence intensity ± 0.04)

Fig. 6 Use of an airfoil to shield the hot-wire sensor.

Fig. 7 Ice accretion on the hot-wire mounting support. (Velocity = $100 \pm 2.5 \text{ mph}$, LWC = $0.7 \pm 0.07 \text{ g/m}^3$, drop size = $20 \pm 0.02 \mu\text{m}$, Total temperature = $25 \pm 2 \text{ }^\circ\text{F}$)

Fig. 8 Turbulence intensity versus nozzle air pressure with zero water pressure at $100 \pm 2.5 \text{ mph}$. (Velocity = $100 \pm 2.5 \text{ mph}$, turbulence intensity ± 0.04 , pressure $\pm 1\%$)

Fig. 9 Turbulence Intensity versus nozzle air pressure for a range of water pressures. (Velocity = $100 \pm 2.5 \text{ mph}$, turbulence intensity ± 0.04 , air pressure $\pm 1\%$, water pressure $\pm 0.05\%$)

Fig. 10 Turbulence intensity versus LWC for a range of droplet sizes. (Velocity = $100 \pm 2.5 \text{ mph}$, turbulence intensity ± 0.04 , LWC $\pm 10\%$, drop size $\pm 10\%$)

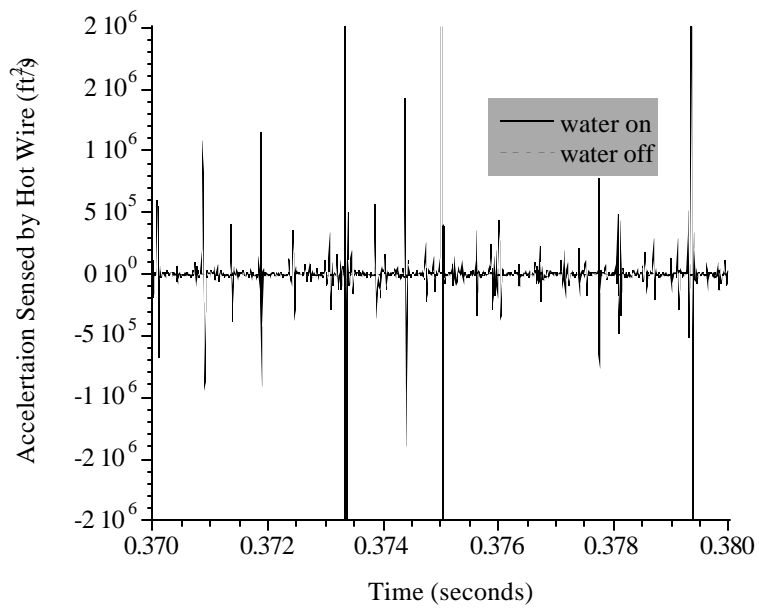
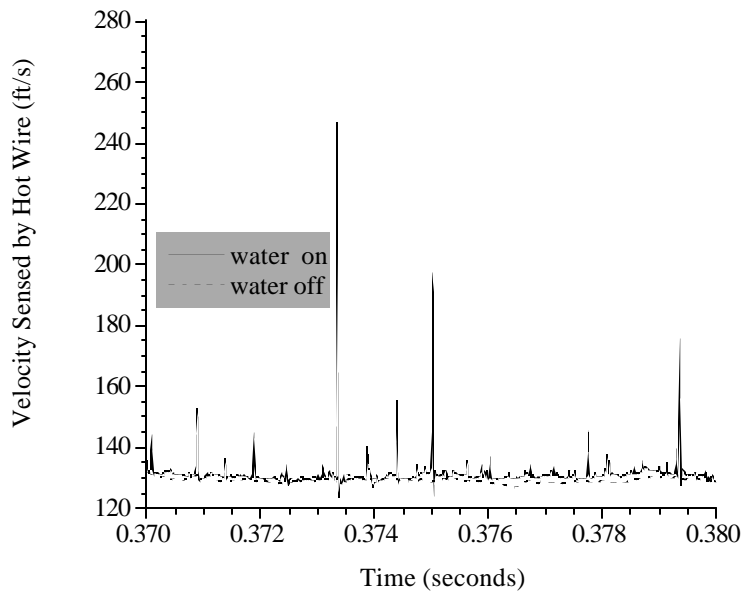


Fig. 1

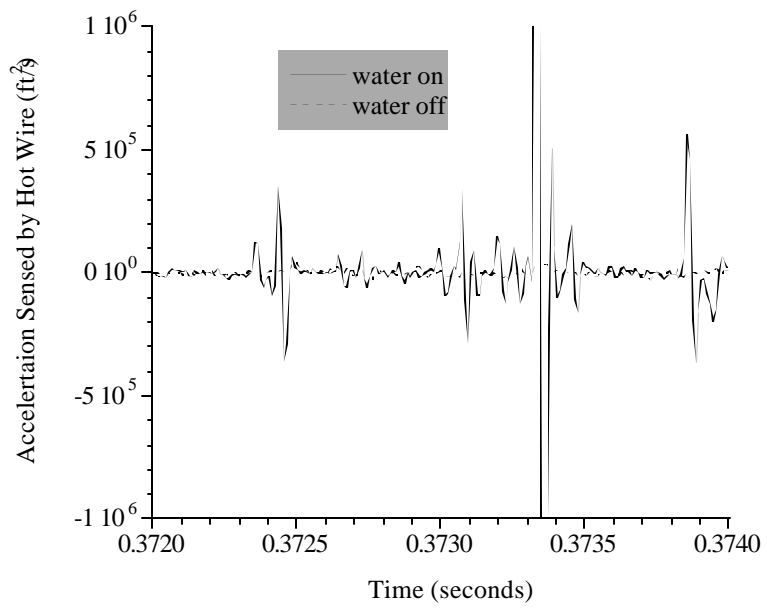
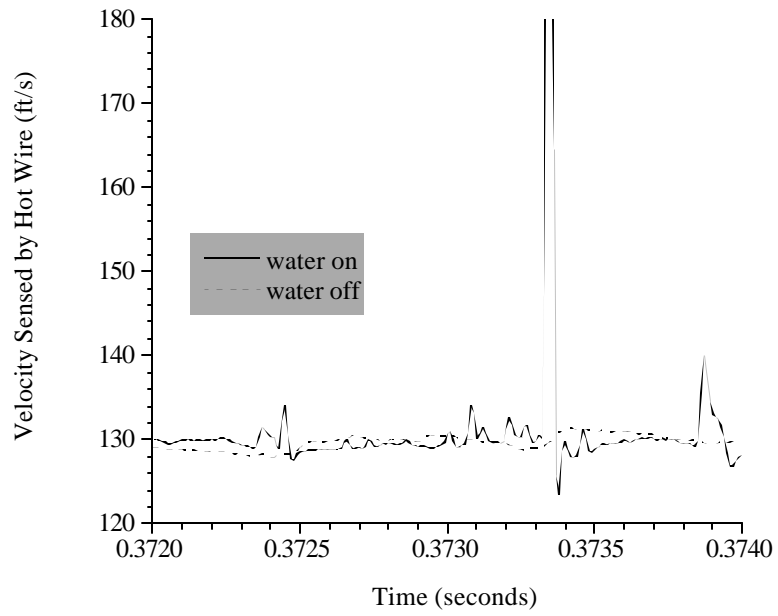


Fig. 2

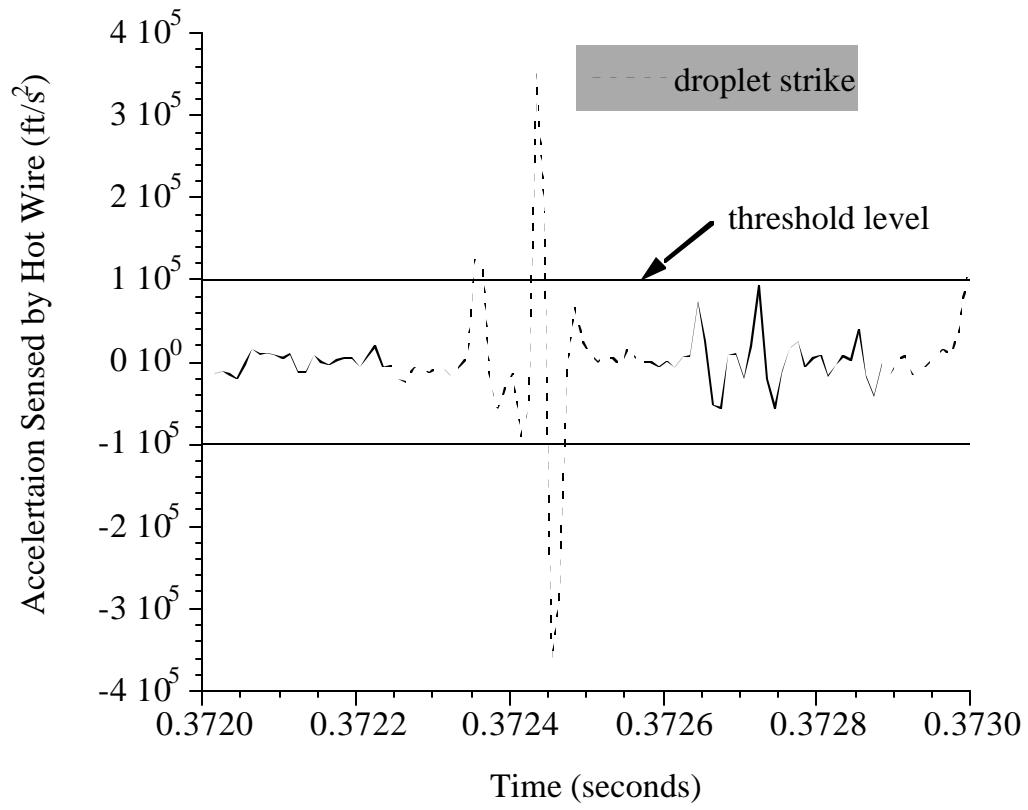


Fig. 3

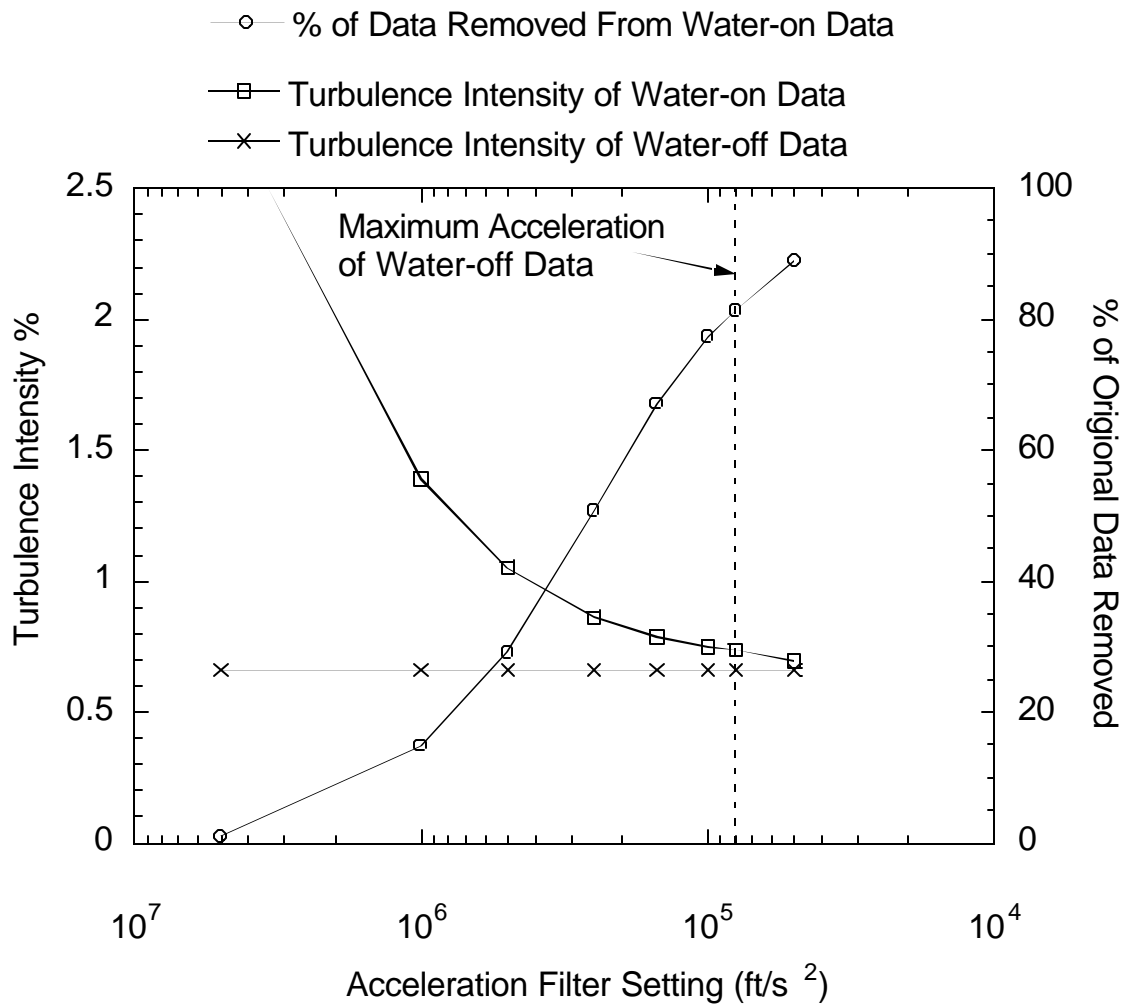


Fig. 4

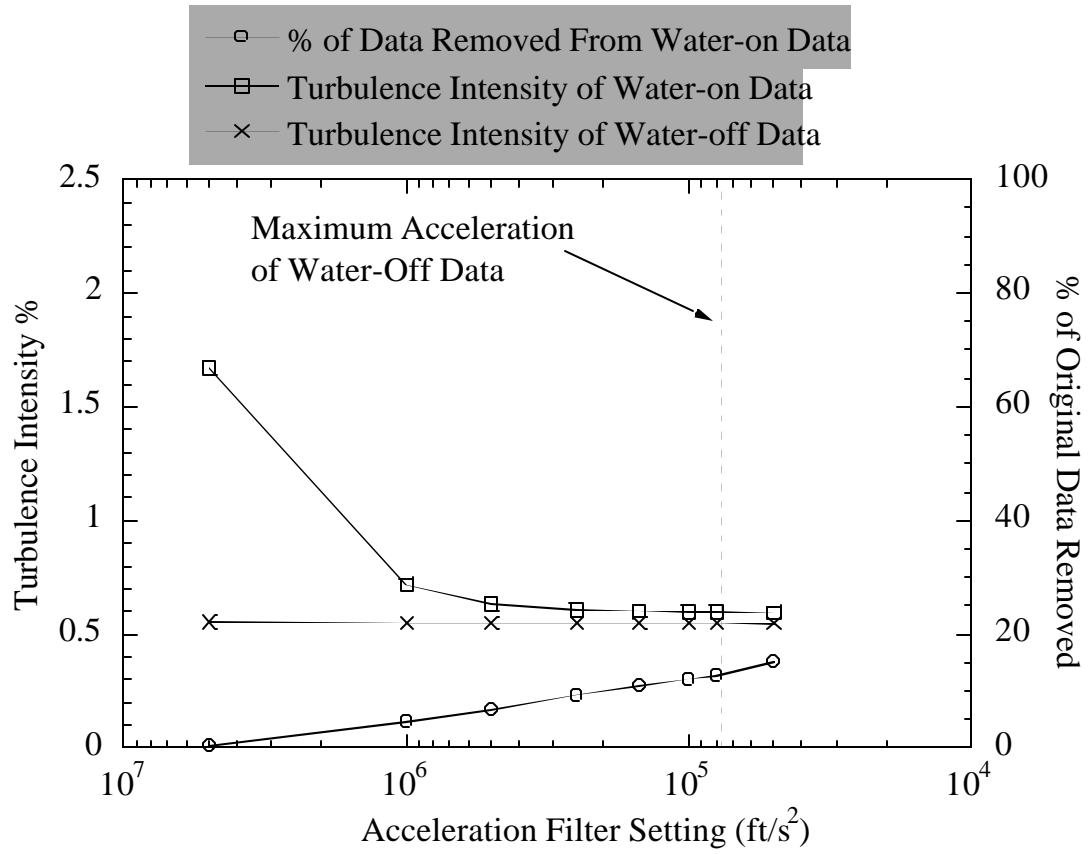


Fig. 5

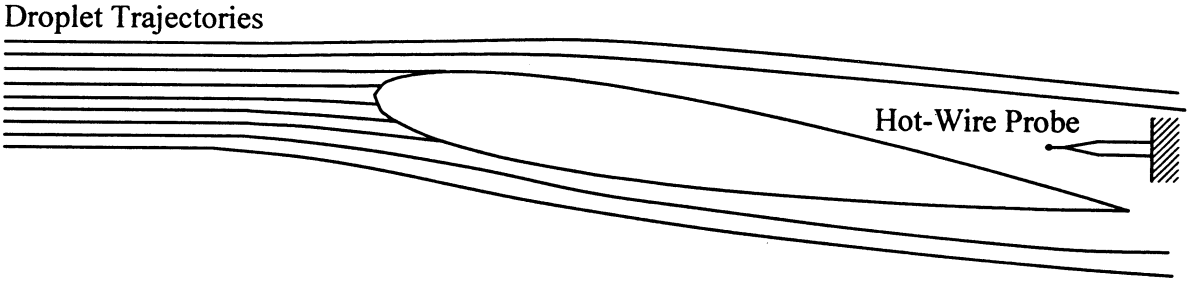


Fig. 6

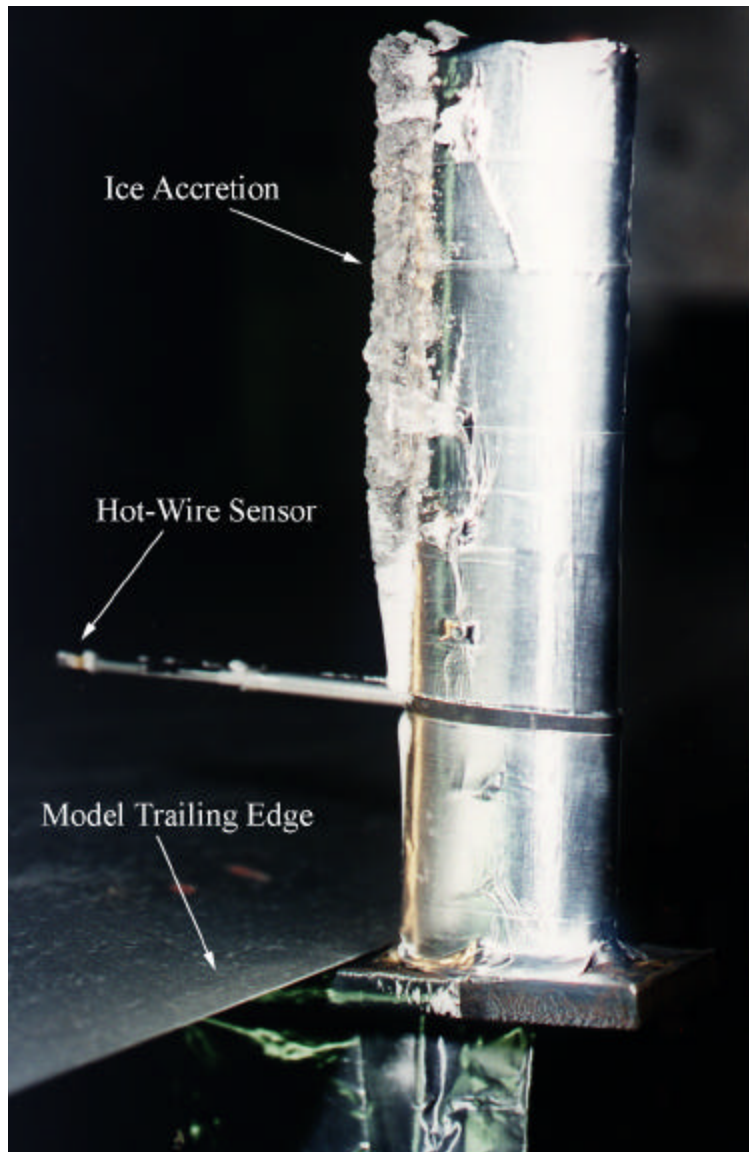


Fig. 7

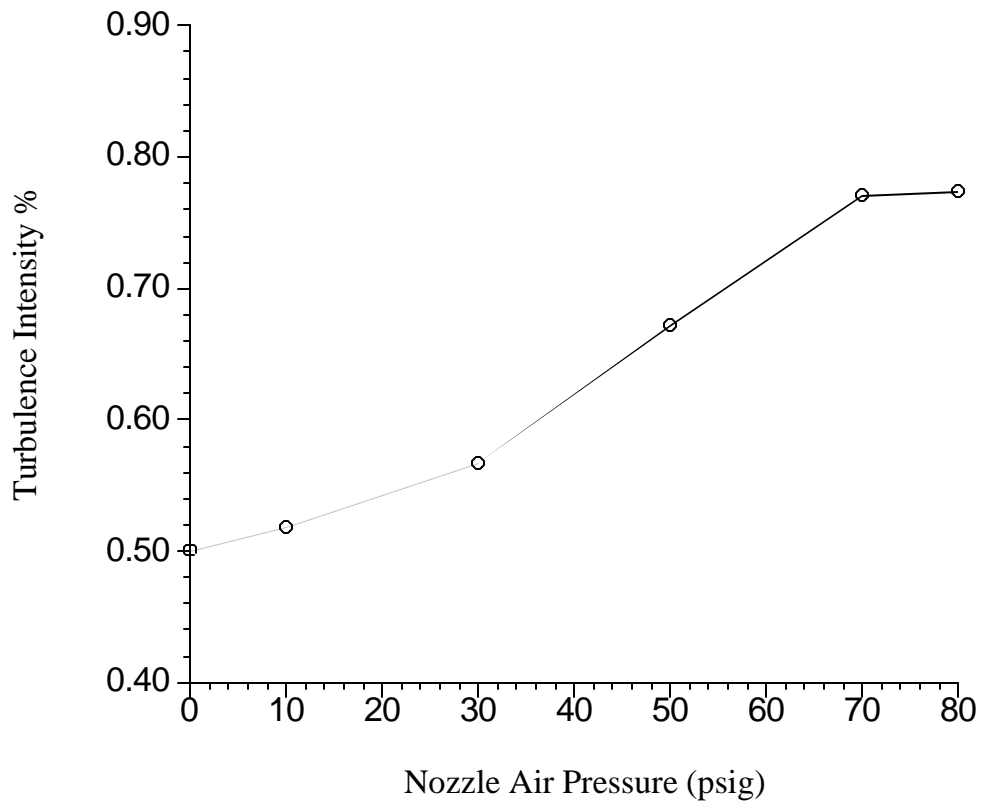


Fig. 8

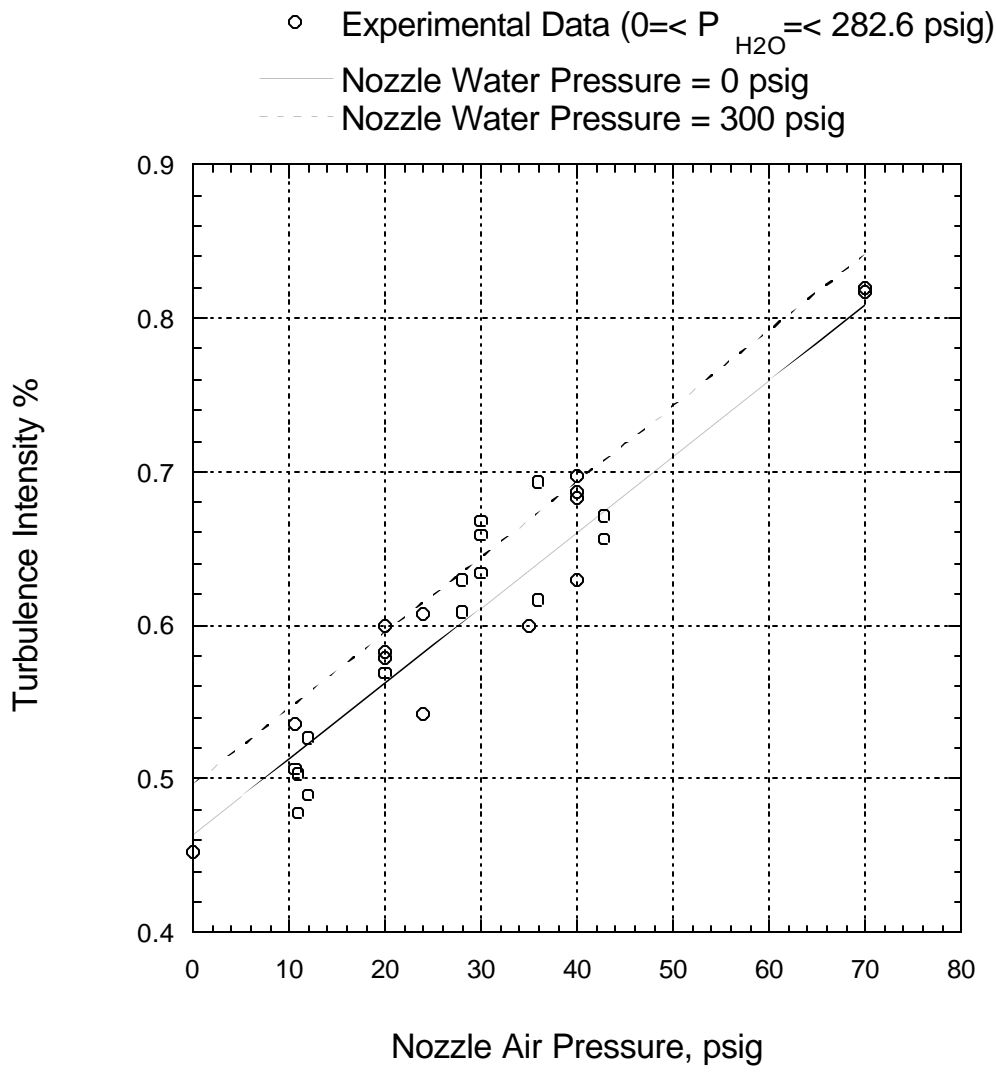


Fig. 9

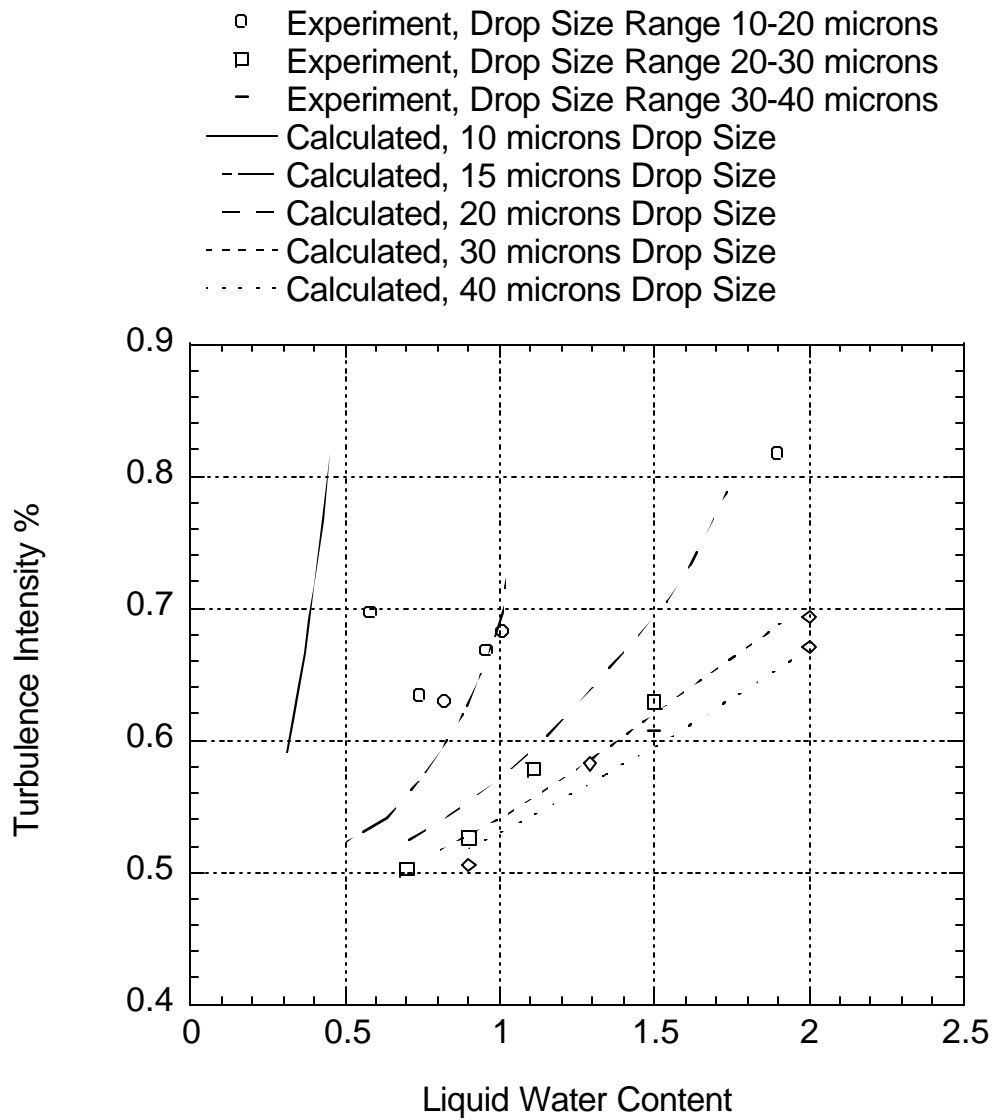


Fig. 10